



UNIVERSITÀ
DEGLI STUDI
FIRENZE

FLORE

Repository istituzionale dell'Università degli Studi di Firenze

Neurokinin-1 receptor blockade and murine lung tumorigenesis.

Questa è la Versione finale referata (Post print/Accepted manuscript) della seguente pubblicazione:

Original Citation:

Neurokinin-1 receptor blockade and murine lung tumorigenesis / Lucattelli M; Fineschi S; P. Geppetti; Gerard NP; Lungarella G. - In: AMERICAN JOURNAL OF RESPIRATORY AND CRITICAL CARE MEDICINE. - ISSN 1073-449X. - STAMPA. - 174:(2006), pp. 674-683.

Availability:

The webpage <https://hdl.handle.net/2158/211149> of the repository was last updated on

Publisher:

American Lung Association:61 Broadway:New York, NY 10006:(212)315-8625, INTERNET: <http://www.>

Terms of use:

Open Access

La pubblicazione è resa disponibile sotto le norme e i termini della licenza di deposito, secondo quanto stabilito dalla Policy per l'accesso aperto dell'Università degli Studi di Firenze (<https://www.sba.unifi.it/upload/policy-oa-2016-1.pdf>)

Publisher copyright claim:

La data sopra indicata si riferisce all'ultimo aggiornamento della scheda del Repository FloRe - The above-mentioned date refers to the last update of the record in the Institutional Repository FloRe

(Article begins on next page)

Neurokinin-1 Receptor Blockade and Murine Lung Tumorigenesis

Monica Lucattelli, Silvia Fineschi, Pierangelo Geppetti, Norma P. Gerard, and Giuseppe Lungarella

Department of Physiopathology, Experimental Medicine, and Public Health, University of Siena, Siena; Department of Critical Care Medicine and Surgery, University of Florence, Florence, Italy; and Department of Pediatrics, Children's Hospital, Harvard Medical School, Boston, Massachusetts

Rationale: Analogous to the adenoma-carcinoma sequence in the colon, it has been proposed that adenocarcinoma (AC) in the lung arises from adenomatous hyperplasia that progresses through atypical adenomatous hyperplasia to AC. However, the data supporting this sequence are largely circumstantial and the almost impossible task of identifying these lesions before resection rules out any longitudinal study in humans.

Objectives, Methods, and Results: We show in mice that the loss of function of the neurokinin-1 receptor (NK-1R)—due to either a pharmacologic or genetic manipulation—results in a sequence of morphologic changes in response to bleomycin treatment that precede the development of AC. We also demonstrate that a series of alterations in gene expression of proliferation markers (i.e., PCNA and Ki-67) and cell cycle regulators (i.e., FHIT, p53, and p21) characterizes the sequence of the precursor lesions. The loss of function of the NK-1R results in changes of the apoptotic rate and in a delay of DNA break recovery of alveolar epithelial cells following bleomycin treatment. The NK-1R blockade interferes with a caspase-independent pathway of apoptosis by affecting both the translocation of Nur77 into the cytoplasm and the expression of some important Bcl2 family members such as Bcl2 and Bak.

Conclusions: To our knowledge, this is the first model to demonstrate a role for NK-1R in lung epithelial cell death and tumorigenesis. This animal model may provide new information on the biology of AC and will facilitate designing and testing of new therapeutic interventions.

Keywords: adenocarcinoma; bleomycin; cell cycle regulators; cell death; proliferation markers

The pulmonary fibrosis in rodents caused by intratracheal administration of a single dose of bleomycin (BLM) is widely used as a model to study the mechanisms of fibrotic lung diseases. Recent evidence has suggested the involvement of tachykinins, and in particular of substance P (SP), in pulmonary fibrosis (1, 2). High levels of immunoreactive SP have been found in bronchoalveolar lavages of patients with idiopathic pulmonary fibrosis and pulmonary sarcoidosis (2). It has been demonstrated that the neuropeptide SP is a potent effector of fibroblast migration and proliferation (3), which in conjunction with other factors (e.g., cytokines, reactive oxygen species) could worsen and accelerate the development of lung fibrosis. In particular, a neuropeptide regulation of proinflammatory and fibrogenic cytokine responses has been

postulated and evidence has been reported demonstrating that SP can induce expression of tumor necrosis factor (TNF)- α (4, 5) and interleukin (IL)-1 (6), two important mediators that can be found at an early stage after BLM treatment. SP released from sensory nerve terminals greatly contributes to neurogenic inflammation mainly by the activation of neurokinin-1 receptors (NK-1R) (7), which are widely expressed in lungs in several cell types including endothelial, epithelial, and smooth muscle cells, monocytes, macrophages, neutrophils, fibroblasts, and mast cells (8–10). NK-1R has recently been shown to be involved in an alternative, programmed cell death (11).

Originally, the aim of the present study was the evaluation of the role of NK-1R in the lung fibrogenic response to BLM in mice treated with a selective NK-1R antagonist. NK-1R blockade did not affect the fibrotic response (either in the fibrosis-prone C57 Bl/6J or in the fibrosis-resistant Balb/c mice: see Figure E1 in the online supplement); however, it resulted in the development of solitary or multiple foci of lung cancer classified as adenocarcinoma (AC) (12) at 21 d after BLM. This finding was unexpected.

To elucidate the specific role of NK-1R signaling in lung tumorigenesis, we used NK-1R knockout (NK1r^{-/-}) mice generated on both C57 Bl/6J and Balb/c backgrounds. This enabled us to observe that (1) the loss of function of the NK-1R results in changes of the apoptotic rate and expression of mediators involved in cell death in response to DNA strand breaks induced by BLM, (2) a sequence of precursor lesions precedes the development of AC, and (3) a series of alterations in gene expression characterizes the precursor lesions, which precede the development of AC.

The almost impossible task of identifying these precursor lesions before resection rules out any longitudinal study in humans. By studying NK1r^{-/-} mice at various times after BLM administration, we were able to demonstrate that AC arises from adenomatous hyperplasia (AH), which progresses through atypical AH (AAH) to AC. The main characteristics of the tumor we report here (i.e., cell of origin, timing of development, morphology of precursor lesions, and histologic and molecular aspects) are quite different from those induced in mice by several carcinogens (13) or by genetic manipulation (i.e., K-Ras conditional mutation) (14–16).

To our knowledge, this is the first model to demonstrate a role for NK-1R in alveolar epithelial cell death and tumorigenesis. Despite the fact that several studies using gene expression profiling have been performed to identify mechanisms of tumor biology in human lung (17–19), a role for NK-1R has not been put forward.

Some of the results of these studies have been previously reported in the form of abstracts (20–22).

METHODS

Animals

Balb/c and C57 Bl/6J mice were supplied by Charles River Italia (Calco, Italy). NK-1R knockout mice (NK1r^{-/-}) were developed by one of us

(Received in original form February 9, 2006; accepted in final form June 20, 2006)

Supported by Ministero dell'Istruzione, dell'Università e della Ricerca, Rome, Italy (MIUR grant 2004067923) and University of Siena, Siena, Italy (PAR grant 2004).

Correspondence and requests for reprints should be addressed to Giuseppe Lungarella, M.D., Department of Physiopathology and Experimental Medicine, University of Siena, via Aldo Moro n.6, 53110 Siena, Italy. E-mail: lungarella@unisi.it

This article has an online supplement, which is accessible from this issue's table of contents at www.atsjournals.org

Am J Respir Crit Care Med Vol 174, pp 674–683, 2006

Originally Published in Press as DOI: 10.1164/rccm.200602-193OC on June 23, 2006
Internet address: www.atsjournals.org

(N.P.G.) at Harvard University, Boston, Massachusetts, as previously described in detail (23) and back-crossed both to Balb/c and C57 Bl/6J mice. The animals were bred at the University of Siena, Siena, Italy. The mice were housed in a light (07:00 to 19:00) and temperature controlled (18 to 22°C) environment, and food (Global Diet 2018; Mucedola, Settimo Milanese, Italy) and water were provided for consumption *ad libitum*. All animal experiments were conducted in conformance with the Guiding Principles for Research Involving Animals and Human Beings and approved by the local ethical committee of the University of Siena, Siena, Italy.

Animal Treatments

A single dose of 150 µg of BLM (Euro Nippon Kayaku GMB, Frankfurt/Main, Germany) in 50 µl saline solution was intratracheally administered to 8- to 16-wk-old male mice of the different strains. All intratracheal instillations were performed under ether anesthesia. Primarily, we evaluated the role of NK-1R in the lung response to BLM in groups of 18 animals for each strain treated with L-733,060 (Merck, Darmstadt, Germany), a selective NK-1R antagonist. It was dissolved in sterile water at a concentration of 16.6 µg/µl and continuously delivered at a rate of 8.3 µg/h for 2 wk by osmotic pumps (Alzet 2002; Alza Corporation, Palo Alto, CA). The pumps were implanted subcutaneously according to the manufacturer's instructions 24 h before BLM treatment. Animals receiving either 50 µl saline or L-733,060 alone served as controls.

Twenty-one days later, the animals from all groups were injected with an overdose of pentobarbital sodium and killed by cutting the abdominal aorta. The lungs were then excised and processed for histologic examination. The evaluation of the fibrotic response was performed by morphometric and biochemical analyses (*see* legend to Figure E1).

Mouse Tumor Analysis

This study was performed using NK1r^{-/-} mice (8 to 16 wk of age) developed on both C57 and Balb/c backgrounds. These animals were used for studying the morphology and the alterations in gene expression characterizing the sequence of precursor lesions that precede AC development.

At 0, 1, 3, 5, 7, 14, 21, and 28 d after BLM treatment, the NK1r^{-/-} mice developed on both C57 and Balb/c backgrounds were killed and the lungs were excised. For conventional light microscopy and immunohistochemistry, lungs were fixed intratracheally with buffered formalin (5%) at a constant pressure of 20 cm H₂O at least for 24 h, dehydrated, cleared in toluene, and embedded in paraffin. Immunohistochemistry was performed using antibodies against Clara cell secretory protein (CCSP), pro-surfactant protein-C, fragile histidine triad (FHIT), proliferation cell nuclear antigen (PCNA), p53, p21, Ki-67, Nur77, and active caspase 3. Samples were also analyzed by terminal deoxynucleotidyl transferase-mediated dUTP-biotin nick-end labeling (TUNEL) technology using the *in situ* Cell Death Detection Kit, Fluorescein (Roche Diagnostics, Basel, Switzerland), according to the manufacturer's recommendations. For biochemistry and RNase protection assay (RPA) analysis, lung samples were processed according to standard procedures. Western blotting was used to analyze activated caspase 3. RPA was performed using multiprobe template sets for analyzing mRNAs for BclW, Bfl1, BclXL, BclXS, Bak, Bax, Bcl2, Bad, and caspases 3, 7, and 8. The distribution of staining was semiquantitatively scored based on the percentage of positive cells: 0, ≤ 5%; 1+, 6–25% stain positive; 2+, 26–50% stain positive; 3+, 51–75% stain positive; and 4+, 76–100% stain positive. The TUNEL labeling index (LI) was scored by determining the average count of the number of cells with positively staining nuclei in airways and epithelial cells. Immunohistochemical examination and TUNEL LI were performed in a blinded fashion by two observers (additional details on the methods and reagents for making these measurements are provided in the online supplement).

Statistical Analysis

For each parameter, either measured or calculated, the values for individual mice were averaged and the SD was calculated. The significance of the differences between groups was calculated using one-way analysis of variance (F-test). A *p* value of less than 0.05 was considered significant.

RESULTS

Pharmacologic Blockade of NK-1R Leads to AC Development after BLM Treatment

All the animals (24 mice; 100% incidence) treated with the selective NK-1R antagonist showed multiple foci of AAH and AC in the peripheral lung parenchyma at 21 d after BLM instillation (Figures 1A and 1B). In these animals, solitary or multiple nodules of parenchymal consolidation are present in the periphery of the lung. The size of these lesions ranges from less than 1 mm to about 3 mm. From a histopathologic point of view, these lesions are characterized by foci of AAH or by well-differentiated alveolar ACs, similar to well-differentiated human ACs (24, 25), but without mucin production or desmoplasia. The foci of AAH are characterized by groups of alveoli distributed around terminal bronchioles, which are well demarcated by pluristratified, plump, cuboidal or low columnar cells with the morphology of type II pneumocytes or Clara cells (Figure 1C, in the *rectangle*). The parenchymal nodules show several areas of frank AC (Figure 1C), which display histologic features of malignancy, such as increased cellularity, nuclear polymorphism including enlarged nuclei with prominent nucleoli, nuclear hyperchromatism, and an increased number of mitotic figures (Figure 1D). In these areas, the tubular arrangement is often completely destroyed due to the cell proliferation. No evidence of stromal, vascular, or pleural invasion was found.

None of these alterations were observed in either Balb/c or C57 Bl/6J mice untreated with the selective NK-1R antagonist after BLM instillation.

Under gross examination, the peripheral nodules can be easily identified on the lung surface in specimens fixed in the inflated state (Figure 1E).

The specific role played by NK-1R in the development of these lesions was investigated in NK1r^{-/-} mice generated on C57 Bl/6J and Balb/c backgrounds. At 21 d after BLM treatment, the same lesions were observed in all NK1r^{-/-} mice (18 of 18) of the different strains (Figures 2A and 2B).

Mice carrying a targeted knockout of NK-1R do not develop spontaneous tumors and in particular lung ACs during their life.

A Sequence of Precursor Lesions Precedes AC Development

NK1r^{-/-} mice with either C57Bl/6 or Balb/c background were used to study the histopathologic changes that precede AC development as well as the alterations in gene expression that characterize the sequence of these histopathologic changes.

Analogous to the adenoma–carcinoma sequence in the colon, it has been proposed that AC arises in the lung from AH, which progresses through AAH to AC (26). By studying NK1r^{-/-} mice at various times after BLM administration, we were able to demonstrate this morphologic sequence in our experimental animals (Figure 3). In particular, AH foci characterized by a monolayer of cuboidal or low columnar cells, which line a group of alveoli, are the predominant lesion between 7 and 14 d after BLM administration (Figure 3B). Between 14 and 21 d after BLM, the predominant lesion is represented by areas of AAH that are recognized as well demarcated foci of epithelial proliferation with some cytologic atypia (Figure 3C). These areas are characterized by a pluristratification of epithelial cells showing enlarged nuclei and hyperchromasia. From 21 d on, the areas of AC predominate (Figure 3D). The latter are well recognized by the presence of columnar, peg-shaped, or cuboidal cells showing an increased mitotic rate and nuclear polymorphism.

In some histologic sections, it is also possible to demonstrate small clusters of cuboidal cells (cuboidal cell hyperplasia; Figure 3A) soon after BLM administration (between 5 and 7 d).

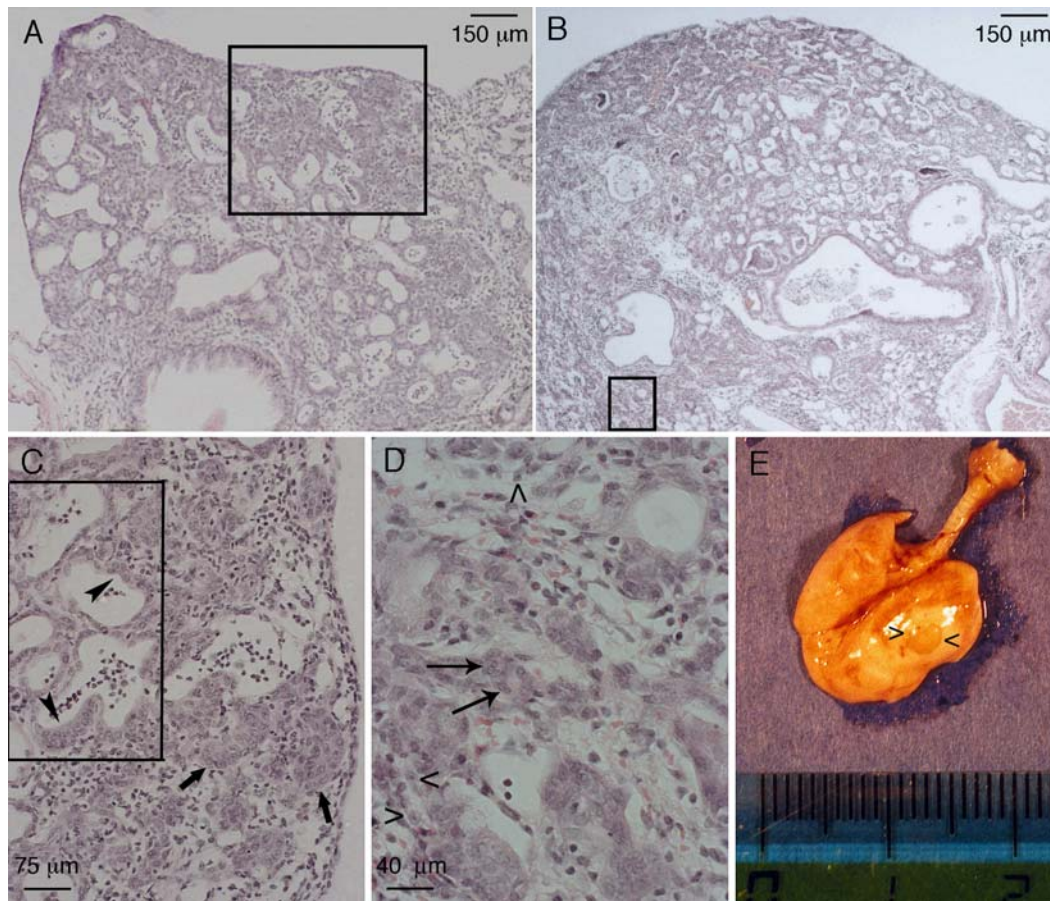


Figure 1. Morphologic appearance of peripheral lung tumors in mice treated with the neurokinin-1 receptor (NK-1R) antagonist L-733,060 at 21 d after treatment with bleomycin (BLM). (A, B) Lung peripheral parenchyma in a C57 Bl/6 mouse (A) and a Balb/c mouse (B) treated with L-733,060, containing areas of atypical adenomatous hyperplasia (AAH) and adenocarcinoma (AC) at 21 d after BLM treatment. Hematoxylin-eosin (H&E) stain. (C) Higher magnification of (A). In the rectangle, note an area of AAH with the characteristic pluristratification of cuboidal or low columnar cells lining alveolar spaces (arrowheads). Some parenchymal nodules show histologic features of malignancy (arrows). H&E stain. (D) Higher magnification of (B). This area of frank AC is characterized by high cellularity, nuclear polymorphism including enlarged nuclei with prominent nucleoli (arrowheads), and an increased number of mitotic figures (arrows). H&E stain. (E) Gross appearance of a peripheral nodule on the surface of a lung fixed at inflated state from a Balb/c mouse treated with L-733,060 at 21 d after BLM.

Alveolar Type II Is the Cell of Origin of AC in $NK1r^{-/-}$ Mice after BLM Treatment

Due to the presence of cell populations resembling type II pneumocytes and Clara cells in the phenotypic traits of precursor lesions (AH and AAH) that characterize the development of ACs, an immunohistochemical approach for identification of specific markers for these cells was used to study the histogenesis

of this tumor. In particular, immunohistochemistry was performed using antibodies against CCSP and the pro-surfactant protein C, commonly used markers that distinguish between Clara cells (Figure 4F) and alveolar type II cells (Figure 4E), respectively. We found that in both AH (Figure 4A) and AAH (Figure 4B), cells stain very strongly for pro-surfactant protein C, but are negative for CCSP (data not shown), whereas in AC

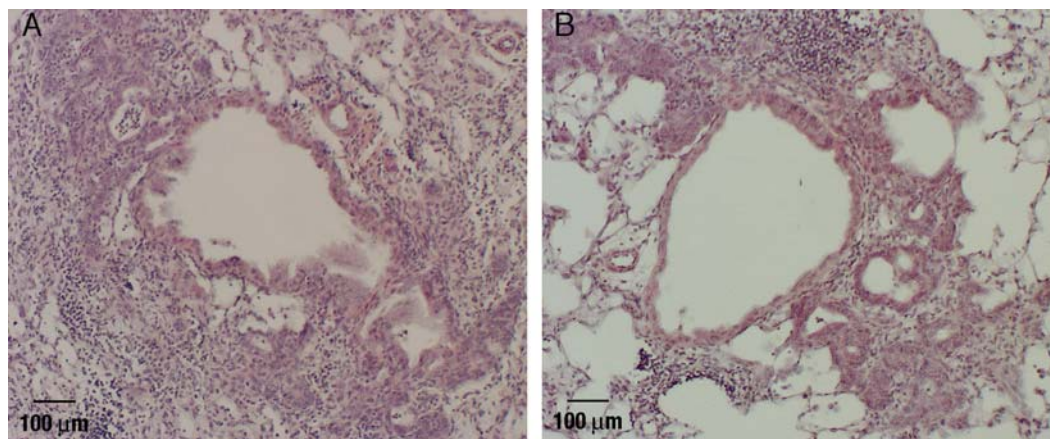


Figure 2. Morphologic appearance of peripheral lung tumors in $NK1r^{-/-}$ mice generated on C57 Bl/6J and Balb/c backgrounds at 21 d after BLM. (A) $NK1r^{-/-}$ mouse (C57 Bl/6J) showing areas of AC and AAH around a bronchiole. H&E stain. (B) $NK1r^{-/-}$ mouse (Balb/c) showing several foci of AC in the periphery of a bronchiole. H&E stain.

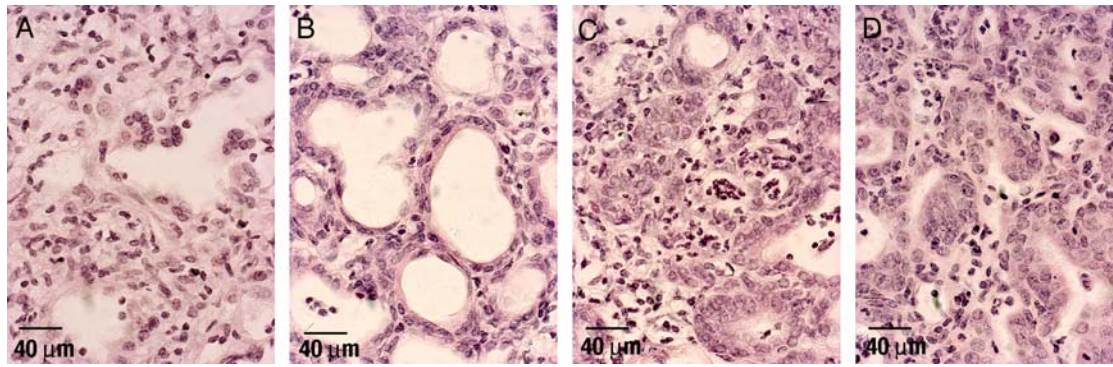


Figure 3. Sequence of adenomatous hyperplasia (AH) to AC in the lungs of $NK1r^{-/-}$ mice after BLM. (A) Small clusters of cuboidal cells (cuboidal cell hyperplasia) in the lung parenchyma of an $NK1r^{-/-}$ Balb/c mouse at 5 d after BLM treatment. (B) Area of AH in the lung of an $NK1r^{-/-}$ Balb/c mouse at 7 d after BLM

treatment. A group of alveoli are lined by a monolayer of cuboidal or low columnar cells. (C) AAH in the lung parenchyma of an $NK1r^{-/-}$ Balb/c mouse at 14 d after BLM. AAH is characterized by a pluristratification of epithelial cells showing enlarged nuclei and hyperchromasia. Scattered inflammatory cells are present. (D) Area of AC in the lung of an $NK1r^{-/-}$ Balb/c mouse at 28 d after BLM treatment showing columnar, peg-shaped, or cuboidal cells with increased mitotic rate and nuclear polymorphism. (A–C) H&E stain.

cells stain less intensely for pro-surfactant protein C (Figure 4C) and are negative for CCSP (Figure 4G). In addition, at 5 to 7 d after BLM treatment, it was possible to demonstrate a general positivity for pro-surfactant protein C (Figure 4D) and no expression of CCSP in small foci of cuboidal cell proliferation.

A Sequence of Alterations in Gene Expression Characterizes the AH to AC Sequence

As mentioned above, a series of precursor lesions characterizes the development of AC in $NK1r^{-/-}$ mice. In particular, foci of AH that progress through AAH to AC are evident in lung parenchyma from 14 to 21 d after BLM treatment. This period has been chosen to study different proliferation markers and cell cycle regulators during the adenoma–carcinoma sequence.

In Figures 5A–5C, the immunohistochemical staining for the tumor suppressor FHIT during the sequence is reported. The data obtained demonstrate a progressive decreasing FHIT expression from AH to AC. On the contrary, staining for PCNA marker (Figures 5D–5F) and Ki67 proliferation marker (Figures 5G–5I) increases during the AH to AC sequence with increasing atypia.

We also examined by immunohistochemistry the interaction between the expression of p53 and of another member of the p53 signaling pathway, namely p53-inducible cyclin-dependent kinase inhibitor p21Waf1/Cip1 (p21). It is well known that p53 and p21 proteins are not usually stained in bronchiolar and epithelial lung cells under normal conditions, but they can be labeled in reactive lesions where a direct correlation between p53 and p21 expression is usually found (27). This correlation is lost during the adenoma–carcinoma sequence under our experimental conditions. In particular, the progressive accumulation of p53 protein we observe during the various progression steps of the AH to AC sequence (Figures 5K–5M) is not matched by an increase of p21 expression. Thus, p21 protein that is highly labeled in AH (Figure 5N) tends to be relatively low in AAH and absent from AC (Figures 5O and 5P). The distribution of the expression of proliferation markers and cell cycle regulators in the adenoma–carcinoma sequence is reported in Table 1.

Loss of Function of NK-1R Does Not Affect Initial Yield of DNA Breaks but Influences Rate of Their Recovery

Representative pictures of DNA strand break (SB) extremities labeling from lung sections of wild-type Balb/c mice at 3 h and

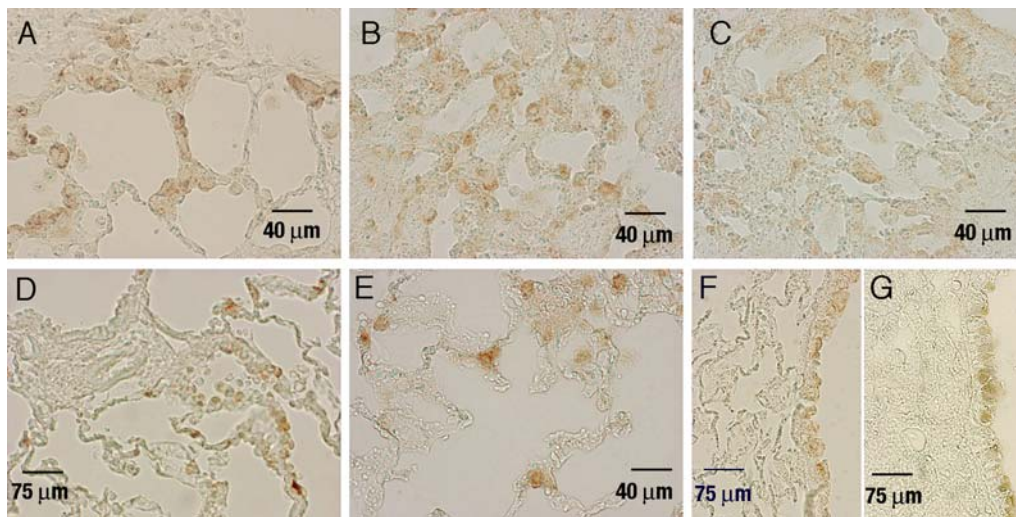


Figure 4. Immunohistochemistry of pro-surfactant protein C (pro-SP-C) and Clara cell secretory protein (CCSP) in the morphologic lesions that characterize the AH to AC sequence. (A) Strong immunostaining for pro-SP-C in foci of AH ($NK1r^{-/-}$ Balb/c mouse at 7 d after BLM treatment). (B) Positive immunostaining for pro-SP-C in epithelial cells of AAH lesion ($NK1r^{-/-}$ Balb/c mouse at 14 d after BLM treatment). (C) Less intense staining for pro-SP-C in AC areas ($NK1r^{-/-}$ Balb/c mouse at 28 d after BLM treatment). (D) Anti-pro-SP-C staining in proliferating cuboidal cells in the parenchyma of a $NK1r^{-/-}$ Balb/c mice at 7 d after BLM treatment. (E) Alveolar

type II cells with positive immunostaining for pro-SP-C in an unaffected area of lung parenchyma. (F) Epithelial cells lining a bronchiole with positive immunostaining for CCSP (lung from a control mouse). (G) Positive immunoreaction for CCSP on bronchiolar epithelial cells. The adjacent area of AC remains negative.

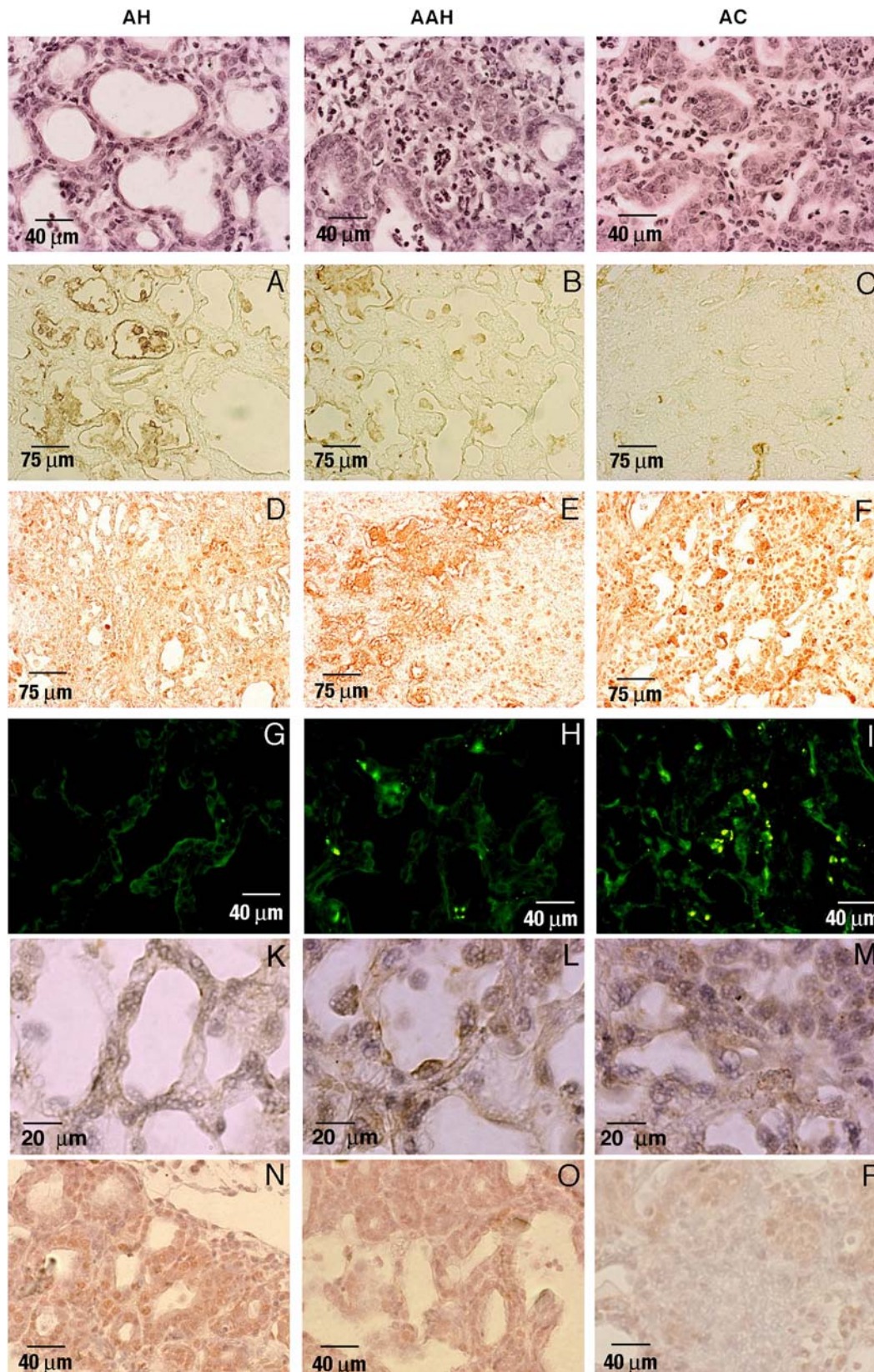


Figure 5. Sequence of alterations in gene expression during the AH-AAH-AC sequence. Immunohistochemical staining for the tumor suppressor fragile histidine triad (A–C), proliferation cell nuclear antigen (PCNA; D–F), Ki67 (G–I), p53 (K–M), and p21 (N–P) during the AH to AC sequence (from left to right). Fragile histidine triad (FHIT) staining and p21 staining (positive cells in brown and brown-red, respectively) show a progressive decreasing expression starting from AH (A, N) to AC (C, P). PCNA (brown-red staining), Ki67 (fluorescent staining), and p-53 (brown staining) show weak (D) or no (G, K) expression in AH. A moderate or strong expression of these proteins is seen in AAH (E, H, L) and AC (F, I, M), respectively.

1, 3, and 5 d after BLM are reported in Figures 6B, 6D, 6F, and 6H, respectively. In these animals, the fluorescein labeling is very strong in epithelial cells of segmental bronchi and bronchioles at 3 h after BLM administration ($LI: 18.5 \pm 10.1$) and less evident

in parenchymal cells ($LI: 4.8 \pm 2.1$; Figure 6B). At 1 d after BLM, a large number of alveolar cells are intensely stained throughout the lung parenchyma (Figure 6D) ($LI: 17.4 \pm 8.5$) when a marked decrease in the labeling of airway epithelial cells

TABLE 1. DISTRIBUTION OF THE EXPRESSION OF PROLIFERATION MARKERS AND CELL CYCLE REGULATORS IN ADENOMATOUS HYPERPLASIA-ADENOCARCINOMA SEQUENCE

		AH					AAH					AC				
		0	1+	2+	3+	4+	0	1+	2+	3+	4+	0	1+	2+	3+	4+
FHIT	n	0	0	8	16		18	6				23	1			
	%			33	66		75	25				96	4			
PCNA	n	2	22					17	7						10	14
	%	8	92					71	29						42	58
Ki67	n	24					14	10				20	4			
	%	100					58	42				83	17			
p53	n	24					11	13				10	14			
	%	100					46	54				42	58			
p21	n			15	9		11	13				19	5			
	%			63	37		46	54				79	21			

Definition of abbreviations: AAH = atypical adenomatous hyperplasia; AC = adenocarcinoma; AH = adenomatous hyperplasia; FHIT = fragile histidine triad; PCNA = proliferation cell nuclear antigen.

Staining distribution (percentage positive cells): 0, \leq 5% staining; 1+, 6–25%; 2+, 26–50%; 3+, 51–75%; and 4+, 76–100% (all reactions exhibited moderate to strong staining intensity).

is found (LI: 4.1 ± 2.7). The fluorescein labeling tends to be relatively low at 3 d after BLM treatment, when only a few cells are positive for SBs (Figure 6F; LI: 6.5 ± 1.9), and absent at 5 d (Figure 6H; LI: 0.6 ± 0.4). The DNA SB labeling for NK1r^{-/-} mice at the various time intervals after BLM administration is shown in Figures 6A, 6C, 6E, and 6G. No appreciable differences in stain distribution (LI) and intensity are observed between knockout and wild-type mice at 3 h (Figure 6A vs. 6B), 1 d (Figure 6C vs. 6D) and 3 d (Figure 6E vs. 6F) after BLM. However, several lung parenchymal cells of NK1r^{-/-} mice still stain at 5 d after BLM administration (LI: 5.1 ± 2.7), when a negative fluorescein labeling is observed for wild-type mice (Figure 6G vs. 6H). These data suggest that the loss function of NK-1R does not influence the initial yield of DNA breaks in response to BLM administration but does result in a delay of DNA SB recovery.

Caspase-dependent Pathways Are Not Significantly Involved in Cell Death after BLM Challenge

Caspase mRNA levels were assessed by RPA in lung tissue from wild-type and NK1r^{-/-} mice at different times after BLM administration. The most significant changes observed at the different times are reported in Figure 6I. Wild-type mice do not show significant changes in the expression of caspases 3, 7, and 8 in comparison with saline-treated control animals at 1 and 3 d after BLM challenge. Unlike wild-type mice, NK1r^{-/-} mice show a significant enhanced expression of caspase 3 (233% increase over control mice) at 1 d after BLM treatment (Figure 6K). In these animals, the expression of caspase 3 increases from 1 d up to 5 d after BLM challenge, reaching the most significant difference from that of control mice at 3 d (466% increase). The presence of active caspase 3 in lung tissue has also been analyzed by Western blotting. Using an enhanced chemiluminescence technique, we were unable to detect any trace of active caspase 3 in tissue samples of NK1r^{-/-} and wild-type mice at 1 and 5 d after BLM administration (data not shown). By immunohistochemistry, very few alveolar cells in alveolar septa of NK1r^{-/-} mice stained with anti-active caspase 3 antibody at various times after BLM challenge (data not shown). The data obtained strongly suggest that, at least at the dosage of BLM used by us, the caspase-dependent pathways—whether mitochondrial-

dependent or receptor-mediated—are not significantly involved in cell death after BLM treatment.

Nur77 and Some Members of the Bcl2 Family Are Implicated in Cell Death after BLM Treatment: Requirement for NK-1R Signaling

The role of nuclear orphan receptor Nur77/TR3 (Nur 77) and of some members of the Bcl2 family in epithelial cell death in response to BLM was investigated in wild-type and NK1r^{-/-} mice at various times after BLM administration. The lung histochemical pattern of Nur77 in mice at 0 and 3 h and at 1 and 3 d after BLM challenge is reported in Figure 7. Under normal conditions, Nur77 protein is not stained in bronchiolar and epithelial lung cells of either genetically engineered or wild-type mice (Figures 7A and 7B). This protein is highly labeled in the cytoplasm of the lower airways and alveolar cells of wild-type mice at 3 h (Figure 7D), 1 d (Figure 7F), and 3 d (Figure 7H) after BLM treatment, but it is absent from lung sections of NK1r^{-/-} mice at the same time points (Figures 7C, 7E, and 7G).

It has been suggested that in response to specific cell death stimuli, including NK-1R signaling (11), Nur77 translocates from the nucleus to the cytoplasm, targeting mitochondria and inducing cytochrome c release (28). In the cytoplasm, Nur77 binds Bcl-2, which subsequently undergoes a conformational change leading to exposure of its BH3 death domain (29). We therefore examined the mRNA expression profile of Bcl2 and other Bcl-2 family members involved in apoptosis by RPA at various times after BLM administration (Figure 7I). A significant increase in the expression of Bak (a proapoptotic Bcl2 family member) and other members with buried BH3 domains (i.e., BclXL, Bcl-2, and BFL1) (30), which can undergo conformational changes after Nur77 binding, is observed in wild-type mice at 3 d after BLM. On the other hand, the only change seen in NK1r^{-/-} mice is an up-regulated expression of BclXL, which usually serves as antiapoptotic molecule in absence of Nur77 (Figure 7I). These data collectively suggest that at least under our experimental conditions Nur77 and some members of the Bcl2 family are implicated in cell death after BLM treatment, and that NK-1R signaling is necessary for the translocation of Nur77 into the cytoplasm and for the expression of some Bcl2 family members involved in apoptosis.

DISCUSSION

In mice, the loss of function of the NK-1R induced either by pharmacologic or genetic manipulation results in the development of AC after BLM administration. The lung tumors are multicentric, well-differentiated ACs, similar to well-differentiated human ACs (24, 25), but without mucin production and desmoplasia.

Analogous to the adenoma–adenocarcinoma sequence in the colon, it has been proposed that AC in humans arises from AH, which progresses through AAH to AC (26). However, the data supporting this sequence in the lung are largely circumstantial and are mainly based on the association of these changes in autopsy studies (31, 32). In our animals, a series of precursor lesions characterize the development of AC. In particular, by studying NK1r^{-/-} mice at various times after BLM administration, we observed (1) several foci of AH in otherwise normal lung parenchyma at 7 and 14 d, (2) a predominance of areas of AAH at 14 to 21 d, and (3) areas of AC sometimes contiguous to foci of AAH from 21 d onwards. We were also able to demonstrate small foci of cuboidal cell hyperplasia at 5 to 7 d after BLM administration and before the occurrence of AH.

The presence of cell population resembling Clara cells within the papillary areas of AC suggested the Clara cell as the cell of origin of these tumors. However, the immunohistochemical

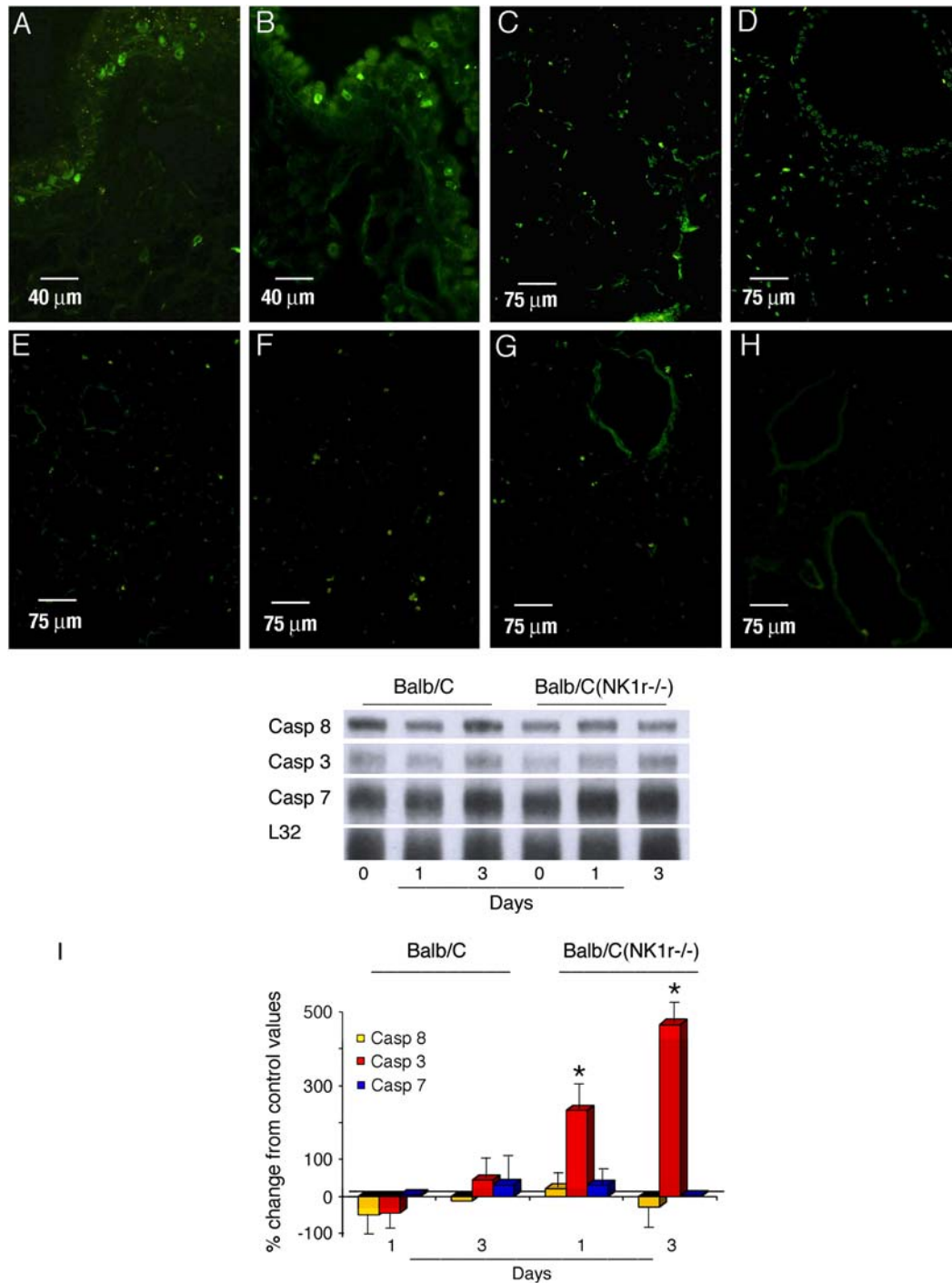


Figure 6. DNA strand-break (SB) extremities labeling and caspase mRNA levels on lung tissues from wild-type and NK1r^{-/-} Balb/c mice after bleomycin (BLM) treatment. (A, C, E, G) DNA SB extremities labeling from lung sections of NK1r^{-/-} mice at 3 h (A) and at 1 (C), 3 (E), and 5 (G) d after BLM. (B, D, F, H) DNA SB extremities labeling from lung sections of wild-type mice at 3 h (B) and at 1 (D), 3 (F), and 5 (H) d after BLM. (I) RNase protection assay (RPA) for caspases after BLM treatment. The data in the graph are mean values \pm SD obtained from three different experiments performed on different pools of three lungs obtained at the various times from wild-type and NK1r^{-/-} Balb/c mice. The gel electrophoretic autoradiographs (I, top) were quantified by Sigma gel analysis software and the values of L 32 were used to normalize the amounts of RNA present in the samples. * $p < 0.05$.

analysis performed by using antibodies against CCSP and pro-surfactant protein C, which are specific markers for Clara and alveolar type II cells respectively, suggests that AC in our mice is of alveolar origin. This conclusion is also supported by the fact that the development of AC is preceded by a series of morphologic lesions bearing cells that stain very strongly for pro-surfactant protein C and are negative for CCSP. Moreover, the absence in these cells of a dual expression of pro-surfactant protein C and CCSP seems to exclude a role for a recently identified bronchioalveolar stem cell as the cell of origin of our neoplasm. This stem cell has been demonstrated to have a role in murine lung epithelial neoplasms that develop in conditional K-Ras mutant mice (16).

Several alterations in gene expression were found to be associated with malignant transformation during the AH to AC sequence in our mice. These alterations are sequential, and their frequency and number increase or decrease with atypia during the AH to AC sequence. In particular, staining for proliferation cell nuclear antigen marker and Ki-67 proliferation marker increases with increasing atypia when a decrease of the tumor suppressor factor FHIT is demonstrated. The latter factor has been involved in tumor initiation and progression of several cancers including those of the lung (33). In addition, the progressive accumulation of p53 expression does not parallel the expression of another member of the p53 signaling pathway, namely p21. This means that the correlation between p53 and p21 (34)

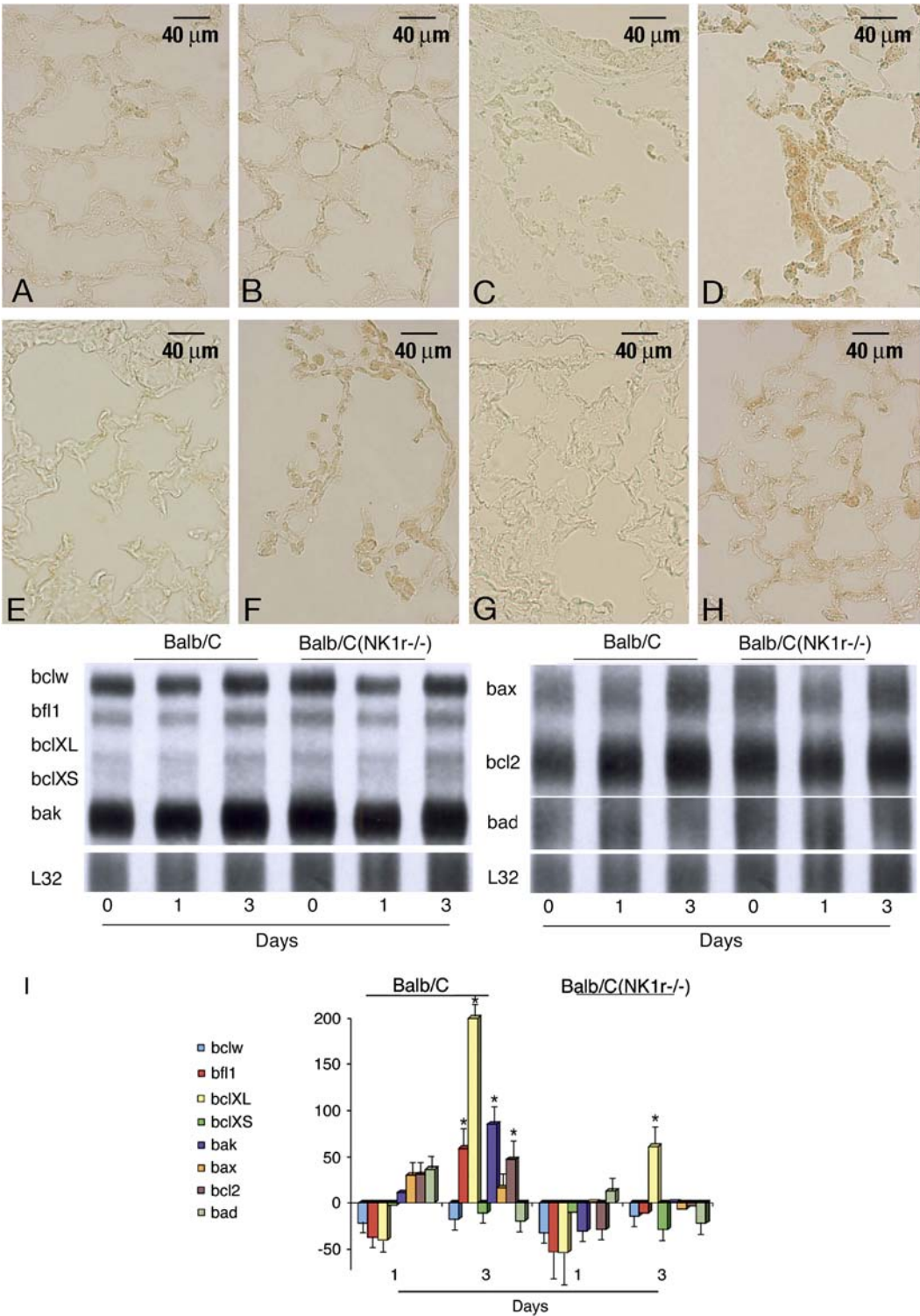


Figure 7. Immunohistochemistry of nuclear orphan receptor Nur77/TR3 (Nur77) and RPA for Bcl2 family members in the lung tissue from wild-type and NK1r^{-/-} Balb/c mice at various times after BLM treatment. (A, C, E, G) Immunostaining for Nur77 in lung sections of NK1r^{-/-} mice at 0 (A) and 3 h (C) and 1 d (E) and 3 d (G) after BLM. (B, D, F, H) Immunostaining for Nur77 in lung sections of wild-type mice at 0 h (B) and 3 h (D) and 1 d (F) and 3 d (H) after BLM. (I) RPA for Bcl2 family members after BLM treatment. The data are mean values ± SD obtained from three different experiments performed on different pools of three lungs obtained at the various times from wild-type and NK1r^{-/-} mice. The gel electrophoretic autoradiographs were quantified by Sigma gel analysis software and the values of L32 were used to normalize the amounts of RNA present in the samples. BLM = bleomycin; RPA = ribonuclease protection assay. bad = *p < 0.05.

is lost during the AH to AC sequence and that p21 expression, which plays an important role in cell cycle regulation, becomes independent during an early stage of transformation. Although p53–p21 uncoupling is extremely frequent and unspecific because p21 may be a target gene of many other factors (e.g., p14ARF and FHIT), it is important to stress that p53–p21 uncoupling has also been reported to characterize the development of the human lung AC (34). The data reported here suggest that hyperproliferation and loss of cell cycle control are early events

in malignant transformation in our model of AH to AC sequence and that a series of alterations in gene expression characterizes the sequence of the histopathologic changes that precede AC development. These alterations can be considered indicative of the preneoplastic nature of these lesions (35, 36). Because mice carrying a targeted knock out of NK-1R do not develop spontaneous tumors and in particular lung ACs during their life, we concluded that NK-1R blockade alone cannot cause neoplastic transformation and hypothesized that a

"secondary" event, namely the BLM-induced DNA damage, is necessary for tumor development and progression. BLM is a radiomimetic anticancer drug that may produce many types of DNA damage including single-strand breaks (SSBs), double-strand breaks (DSBs), base damage, and DNA-DNA or DNA-protein cross-links (37). Depending on the drug concentration reached in the cell, BLM can induce different types of DNA breaks (SSBs or DSBs) in the injured tissues (38). These changes undergo repair or can induce cell death by caspase-dependent (SSB) or caspase-independent (DSB) apoptosis pathways (39). Low concentrations of BLM in the cell generally induce SSBs, whereas high concentrations result in a high prevalence of DSBs (38). Thus, under *in vivo* conditions, the prevalence of these changes may vary on the basis of the dose of BLM used and the route of administration.

Of the various forms of damage that are inflicted by BLM, probably the most dangerous is the DSB. Inaccurate repair or lack of repair of a DSB can lead to mutations or to a larger scale genomic instability through the generation of dicentric or acentric chromosomal fragments. Such genomic changes may have tumorigenic potential (39). Thus, DSBs are potent inducers of mutations and of cell death. However, the intracellular cell death pathways that are activated on direct exposure of BLM to alveolar epithelial cells remain to be clarified.

To investigate the role of the NK-1R blockade on the development of AC, we studied the different kinetics in the generation and disappearance of DNA breaks in wild-type and NK1r^{-/-} mice after BLM challenge. The loss of function of NK-1R does not influence the initial yield of DNA breaks in response to BLM administration but does result in a delay of DNA break recovery. This led us to hypothesize that defects in cellular response to DNA SBs (e.g., inappropriate DSB repair events, difficulty of cells to undergo apoptosis/cell death, or both) that are generally recognized as a frequent initiating event in carcinogenesis (40, 41) could be favored by the NK-1R blockade.

Because the exact role of DNA breaks in the triggering of cell death is far from being well established, we evaluated the contribution of the caspase-dependent pathways, Nur77, and some members of the Bcl2 family in the epithelial cell death in response to BLM in both wild-type and NK1r^{-/-} mice.

NK-1R has recently been shown to be involved in an alternative, programmed cell death. NK-1R death signaling is dependent on arrestin 2-mediated activation of MAPK phosphorylation cascade integrated by Raf-1-MEK2-ERK2, leading to the phosphorylation of Nur77, the downstream effector of ERK2 activation (11). Nur77 translocates from the nucleus to the mitochondria, to trigger cytochrome c release and apoptosis (28). Recent evidence suggests that Nur77 targets mitochondria through its interaction with Bcl-2. In particular, Bcl-2 containing buried BH3 death domain may be converted from protector to killer by interaction with Nur77 (29).

The data obtained from wild-type mice support the idea that, at least under our experimental conditions, Nur77 and some members of the Bcl2 family are key regulators of the cell death pathway after BLM exposure in alveolar epithelial cells. On the contrary, the caspase-dependent pathways (either mitochondrial-dependent or receptor-mediated) are not significantly involved. The NK-1R blockade seems to interfere with this caspase-independent pathway of apoptosis by affecting both the translocation of Nur77 into the cytoplasm and the expression of some important Bcl2 family members. These data strongly suggest that the delay of DNA break recovery seen in NK1r^{-/-} mice after BLM challenge is due to ineffective activation of the non-apoptotic cell death pathway that involves Nur 77 and some Bcl2 family members such as Bcl2 and Bak (14). On the other hand, we cannot exclude the possibility that the loss of NK-1R

results in a gain of function (i.e., changes in p53 or other important transcription factors) that could confer a dominant negative status inhibiting the activation of p21.

In conclusion, although much more work is necessary to clarify the molecular mechanisms that lead to the development of AC under our experimental conditions, the observations reported in this study open the way to identifying the signaling pathways crucial for AC and the molecular characteristics of the precursor lesions. The almost impossible task of identifying these lesions before resection rules out any longitudinal study in humans. Our animal model of AC may facilitate designing and testing of new therapeutic interventions against peripheral human ACs and provide new information on the biology of AC and on potential targets for detection and possibly even treatment.

Conflict of Interest Statement: None of the authors has a financial relationship with a commercial entity that has an interest in the subject of this manuscript.

References

1. Brunelleschi S, Nicali R, Lavagno L, Viano I, Pozzi E, Gagliardi L, Ghio P, Albera C. Tachykinin activation of human monocytes from patients with interstitial lung disease, healthy smokers or healthy volunteers. *Neuropptides* 2000;34:45-50.
2. Takeyama M, Nagai S, Mori K, Ikawa K, Satake N, Izumi T. Substance P-like immunoreactive substance in bronchoalveolar lavage fluids from patients with idiopathic pulmonary fibrosis and pulmonary sarcoidosis. *Sarcoidosis Vasc Diffuse Lung Dis* 1996;13:33-37.
3. Harrison NK, Dawes KE, Kwon OJ, Barnes PJ, Laurent GJ, Chung KF. Effects of neuropeptides on human lung fibroblast proliferation and chemotaxis. *Am J Physiol* 1995;268:L278-L283.
4. Okabe T, Hide M, Koro O, Yamamoto S. Substance P induces tumor necrosis factor- α release from human skin via mitogen-activated protein kinase. *Eur J Pharmacol* 2000;398:309-315.
5. Ho WZ, Stavropoulos G, Lai JP, Hu BF, Magafa V, Anagnostides S, Douglas SD. Substance P C-terminal octapeptide analogues augment tumor necrosis factor- α release by human blood monocytes and macrophages. *J Neuroimmunol* 1998;82:126-132.
6. Bahl AK, Foreman JC. Stimulation and release of interleukin-1 from peritoneal macrophages of the mouse. *Agents Actions* 1994;42:154-158.
7. Geppetti P, Holzer P. Neurogenic inflammation. Boca Raton, FL: CRC Press; 1996.
8. O'Connor TM, O'Connell J, O'Brian DI, Goode T, Bredin CP, Shanahan F. The role of substance P in inflammatory disease. *J Cell Physiol* 2004;201:167-180.
9. Bai TR, Zhou D, Weir T, Walker B, Hegele R, Hayashi S, McKay K, Bondy GP, Fong T. Substance P (NK1)- and neurokinin A (NK2)-receptor gene expression in inflammatory airway diseases. *Am J Physiol* 1998;269:L309-L317.
10. Strigas J, Burcher E. Autoradiographic localization of tachykinin NK2 and NK1 receptors in the guinea-pig lung, using selective radioligands. *Eur J Pharmacol* 1996;311:177-186.
11. Castro-Obrégón S, Rao RV, del Rio G, Chen SF, Poksay KS, Rabizadeh S, Vesce S, Zhang X-K, Swanson RA, Bredesen DE. Alternative, nonapoptotic programmed cell death: mediation by Arrestin 2, ERK2, and Nur77. *J Biol Chem* 2004;279:17543-17553.
12. Nikitin AY, Alcaraz A, Anver MR, Bronson RT, Cardiff RD, Dixon D, Fraire AE, Gabrielson EW, Gunning WT, Haines DC *et al.* Classification of proliferative pulmonary lesions of the mouse: recommendations of the mouse models of Human Cancer Consortium. *Cancer Res* 2004;64:2307-2316.
13. Malkinson AM. Primary lung tumors in mice as an aid for understanding, preventing, and treating human adenocarcinoma of the lung. *Lung Cancer* 2001;32:265-279.
14. Jackson EL, Willis N, Mercer K, Bronson RT, Crowley D, Montoya R, Jacks T, Tuveson DA. Analysis of lung tumors initiation and progression using conditional expression of oncogenic K-ras. *Genes Dev* 2001;15:3243-3248.
15. Fisher GH, Wellen SL, Klimstra D, Lenczowski JM, Tichelaar JW, Lizak MJ, Whitsett JA, Koretsky A, Varmus HE. *Genes Dev* 2001;15:3249-3262.
16. Bender Kim CF, Jackson EL, Woolfenden AE, Lawrence S, Babar I, Vogel S, Crowley D, Bronson RT, Jacks T. Identification of bronchioalveolar stem cells in normal lung and lung cancer. *Cell* 2005;121:823-835.

17. Hofmann HS, Hansen G, Burdach S, Bartling B, Silber RE, Simm A. Discrimination of human lung neoplasm from normal lung by two target genes. *Am J Respir Crit Care Med* 2004;10:516–519.
18. Borczuk AC, Kim HK, Yegen HA, Friedman RA, Powell CA. Lung adenocarcinoma global profiling identifies type II transforming growth factor β receptor as a repressor of invasiveness. *Am J Respir Crit Care Med* 2005;172:729–737.
19. Jett JR, Miller YE. Update in lung cancer 2005. *Am J Respir Crit Care Med* 2006;173:695–697.
20. Lucattelli M, Fineschi S, Geppetti P, Lungarella G. Role of the Nk-1 receptor in the development of non-small cell carcinoma in bleomycin treated mice [abstract]. *Proc Am Thorac Soc* 2005;2:A899.
21. Lucattelli M, Fineschi S, Geppetti P, Gerard NP, Lungarella G. The loss of function of NK-1 receptor in mice results in the development of bronchiolo-alveolar carcinoma after bleomycin treatment [abstract]. *FASEB J* 2006;20:A1328.
22. Lucattelli M, Fineschi S, Geppetti P, Gerard NP, Lungarella G. An animal model for studying the sequence of precursor lesions that characterize the development of bronchiolo-alveolar carcinoma [abstract]. *Proc Am Thorac Soc* 2006;3:A479.
23. Bozic CR, Lu B, Hopken UE, Gerard C, Gerard NP. Neurogenic amplification of immune complex inflammation. *Science* 1996;273:1722–1725.
24. Thurlbeck WM, Miller RR. The respiratory system. In: Rubin E, Farber JL, editors. Pathology. Philadelphia, PA: Lippincott; 1988. pp. 542–627.
25. Travis WD, Brambilla E, Müller-Hermelink HK, Harris CC. WHO Classification of tumours: pathology & genetics of tumours of the lung, pleura, thymus and heart. Lyon, France: IARC Press; 2004.
26. Miller RR, Nelems B, Evans KG, Muller NL, Ostrow DN. Glandular neoplasia of the lung: a proposed analogy to colonic tumors. *Cancer* 1988;61:1009–1014.
27. Guinee D Jr, Fleming M, Hayashi T, Woodward M, Zhang J, Walls J, Koss M, Ferrans V, Travis W. Association of p53 and WAF1 expression with apoptosis in diffuse alveolar damage. *Am J Pathol* 1996;149:531–538.
28. Li H, Kolluri SK, Gu J, Dawson MI, Cao X, Hobbs PD, Lin B, Chen G, Lu J, Lin F, *et al.* Cytochrome c release and apoptosis induced by mitochondrial targeting of nuclear orphan receptor TR3. *Science* 2000;289:1159–1164.
29. Lin B, Kolluri SK, Lin F, Liu W, Han Y-H, Cao X, Dawson MI, Reed JC, Zhang X-K. Conversion of Bcl-2 from protector to killer by interaction with Nuclear Orphan receptor Nur77/TR3. *Cell* 2004;116:527–540.
30. Gross A, McDonnell JM, Korsmeyer SJ. BCL-2 family members and the mitochondria in apoptosis. *Genes Dev* 1999;13:1899–1911.
31. Kerr KM. Pulmonary preinvasive neoplasia. *J Clin Pathol* 2001;54:257–271.
32. Greenberg AK, Yee H, Rom WL. Preneoplastic lesions of the lung. *Respir Res* 2002;3:20–29.
33. Carpagnano GE, Foschino-Barbaro MP, Mulè G, Resta O, Tommasi S, Mangia A, Carpagnano F, Stea G, Susca A, Di Gioia G, *et al.* 3p microsatellite alterations in exhaled breath condensate from patients with non-small cell lung cancer. *Am J Respir Crit Care Med* 2005;172:738–744.
34. Hayashi H, Miyamoto H, Ito T, Kameda Y, Nakamura N, Kubota Y, Kitamura H. Analysis of p21Awf1/Cip1 expression in normal, premalignant, and malignant cells during the development of human lung adenocarcinoma. *Am J Pathol* 1997;151:461–470.
35. Bartkova J, Horejsi Z, Koed K, Kramer A, Tort F, Zieger K, Guldberg P, Sehested M, Nesland JM, Lukas C, *et al.* DNA damage response as a candidate anti-cancer barrier in early human tumorigenesis. *Nature* 2005;434:864–870.
36. Gorgoulis VG, Vassiliou LVF, Karakaidos P, Zacharatos P, Kotsinas A, Liloglou T, Venere M, DiTullio RA Jr, Kastrinakis NG, Levy B, *et al.* Activation of the DNA damage checkpoint and genomic instability in human precancerous lesions. *Nature* 2005;434:907–913.
37. Cole A, Meyn RE, Chen R, Corry PM, Hillelman W. Mechanisms of cell injury. In: Meyn RE, Withers HR, editors. Radiation biology in cancer research. New York, NY: Raven Press Ltd; 1980. pp. 33–58.
38. Mekid H, Tounekti O, Spatz A, Cemazar M, El Kebir FZ, Mir LM. In vivo evolution of tumour cells after the generation of double-strand DNA breaks. *Br J Cancer* 2003;88:1763–1771.
39. Jackson SP. Sensing and repairing DNA double strand breaks. *Carcinogenesis* 2002;23:687–696.
40. van Gent DC, Hoeijmakers JHJ, Kanaar R. Chromosomal stability and the DNA double-strand break connection. *Nat Rev Genet* 2001;2:196–206.
41. Khanna KK, Jackson SP. DNA double-strand breaks: signalling, repair and the cancer connection. *Nat Genet* 2001;27:247–254.